

AD-A203 913

NCEL

Contract Report

CR 89.002

November 1988

An Investigation Conducted By
University of California at Davis

Sponsored By Naval Facilities
Engineering Command

FILE COPY

THE APPLICATION OF MODAL COORDINATE METHODS TO LARGE NONLINEAR TIME-DEPENDENT PROBLEMS

ABSTRACT The research presented in this document demonstrates the application of a modal projection scheme based on inverse Lanczos iteration to a variety of problems in computational mechanics. All the cases considered are nonlinear and time-dependent, and Lanczos vectors are used to achieve coordinate reductions that substantially reduce the sizes of the underlying problems. Varying degrees of success are encountered in these reductions, depending upon numerical characteristics of the original Finite-Element models. A review of the theory of modal projection methods is presented in order to explain the results of the reduced coordinate approximations.

DTIC
ELECTE
JAN 26 1989
S a D

89 1 26 048

NAVAL CIVIL ENGINEERING LABORATORY, FORT HUENEME, CALIFORNIA 93043

METRIC CONVERSION FACTORS

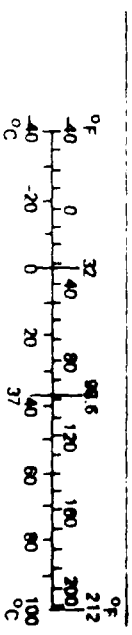
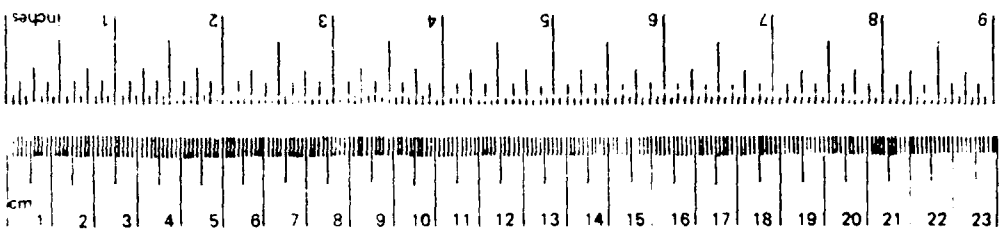
Approximate Conversions to Metric Measures

Symbol	When You Know	Multiply by	To Find	Symbol
in ft yd mi	inches	2.5	centimeters	cm
	feet	30	centimeters	cm
	yards	0.9	meters	m
	miles	1.6	kilometers	km
in ² ft ² yd ² mi ²	square inches	6.5	square centimeters	cm ²
	square feet	0.09	square meters	m ²
	square yards	0.8	square meters	m ²
	square miles	2.6	square kilometers	km ²
	acres	0.4	hectares	ha
oz lb	ounces	28	grams	g
	pounds	0.45	kilograms	kg
	short tons	0.9	tonnes	t
	(2,000 lb)			
tsp tbsp fl oz c pt qt gal ft ³ yd ³	teaspoons	5	milliliters	ml
	tablespoons	15	milliliters	ml
	fluid ounces	30	milliliters	ml
	cups	0.24	liters	l
	pints	0.47	liters	l
	quarts	0.95	liters	l
	gallons	3.8	liters	l
	cubic feet	0.03	cubic meters	m ³
	cubic yards	0.76	cubic meters	m ³
TEMPERATURE (exact)				
°F	Fahrenheit temperature	5/9 (after subtracting 32)	Celsius temperature	°C

* 1 in. = 2.54 (exactly). For other exact conversions and more detailed tables, see NBS Metric Publ. 286, *Units, Weights and Measures*, Price \$2.75, SD Catalog No. C13 10 286.

Approximate Conversions from Metric Measures

Symbol	When You Know	Multiply by	To Find	Symbol
mm cm m km	millimeters	0.04	inches	in
	centimeters	0.4	inches	in
	meters	3.3	feet	ft
	kilometers	1.1	yards	yd
		0.6	miles	mi
cm ² m ² km ²	square centimeters	0.16	square inches	in ²
	square meters	1.2	square yards	yd ²
	square kilometers	0.4	square miles	mi ²
	hectares (10,000 m ²)	2.5	acres	
AREA				
g kg t	grams	0.035	ounces	oz
	kilograms	2.2	pounds	lb
	tonnes (1,000 kg)	1.1	short tons	
ml l m ³	milliliters	0.03	fluid ounces	fl oz
	liters	2.1	pints	pt
	liters	1.06	quarts	qt
	cubic meters	0.26	gallons	gal
	cubic meters	35	cubic feet	ft ³
	cubic meters	1.3	cubic yards	yd ³
TEMPERATURE (exact)				
°C	Celsius temperature	9/5 (then add 32)	Fahrenheit temperature	°F



Unclassified

ADA203913

SECURITY CLASSIFICATION OF THIS PAGE (When Data Entered)

REPORT DOCUMENTATION PAGE		READ INSTRUCTIONS BEFORE COMPLETING FORM
1 REPORT NUMBER CR 89.002	2 GOVT ACCESSION NO.	3 RECIPIENT'S CATALOG NUMBER
4 TITLE (and Subtitle) The Application of Modal Coordinate Methods to Large Nonlinear Time- Dependent Problems		5 TYPE OF REPORT & PERIOD COVERED Final Jan 1988 - Sep 1988
7 AUTHOR(s) Kyran D. Mish Leonard R. Herrmann		6 PERFORMING ORG. REPORT NUMBER
9 PERFORMING ORGANIZATION NAME AND ADDRESS The University of California at Davis		8 CONTRACT OR GRANT NUMBER(s) N62583-87MT227
11 CONTROLLING OFFICE NAME AND ADDRESS Naval Civil Engineering Laboratory Port Hueneme, CA 93043-5003		10 PROGRAM ELEMENT, PROJECT, TASK AREA & WORK UNIT NUMBERS 61153N YR023.03.01.008
14 MONITORING AGENCY NAME & ADDRESS (if different from Controlling Office) Naval Facilities Engineering Command 200 Stovall Street Alexandria, VA 22332-2300		12 REPORT DATE November 1988
		13 NUMBER OF PAGES 48
		15 SECURITY CLASS. (of this report) Unclassified
		15a. DECLASSIFICATION/DOWNGRADING SCHEDULE
16 DISTRIBUTION STATEMENT (of this Report) Approved for public release; distribution is unlimited		
17 DISTRIBUTION STATEMENT (of the abstract entered in Block 20, if different from Report)		
18 SUPPLEMENTARY NOTES		
19 KEY WORDS (Continue on reverse side if necessary and identify by block number) Nonlinear finite element analysis, solution algorithms, eigen- vectors, Ritz vectors, Lanczos vectors, modal analysis		
20 ABSTRACT (Continue on reverse side if necessary and identify by block number) The research presented in this document demonstrates the application of a modal projection scheme based on inverse Lanczos iteration to a variety of problems in computational mechanics. All the cases considered are nonlinear and time- dependent, and Lanczos vectors are used to achieve coordinate reductions that substantially reduce the sizes of the under-		

Unclassified

SECURITY CLASSIFICATION OF THIS PAGE (When Data Entered)

Unclassified

SECURITY CLASSIFICATION OF THIS PAGE(When Data Entered)

lying problems. Varying degrees of success are encountered in these reductions, depending upon numerical characteristics of the original Finite-Element models. A review of the theory of modal projection methods is presented in order to explain the results of the reduced coordinate approximations.

Accession For	
NTIS GRA&I	<input checked="checked" type="checkbox"/>
DTIC TAB	<input type="checkbox"/>
Unannounced	<input type="checkbox"/>
Justification	
By	
Distribution/	
Availability Codes	
Avail and/or	
Dist Special	
A-1	

Unclassified

SECURITY CLASSIFICATION OF THIS PAGE(When Data Entered)



The Application of Modal Coordinate Methods to Large Nonlinear Time-Dependent Problems

Table of Contents

Chapter	Topic	Page
<u>Introduction</u>		1
<u>Review of Previous Work</u>		2
	The Projection Theorem	2
	Eigenvector Expansion Methods	4
	Krylov Subspace Methods	6
<u>Example Applications</u>		9
	Bounding-Surface Soil Dynamics	9
	Nonlinear Flow in a Porous Media	15
	Soil Dynamics Incorporating Porewater Effects	23
<u>Extensions</u>		26
	Suggestions for Further Study	26
	Conclusions	27
	References	28

Chapter 1

Introduction

Introduction

There are always interesting problems in engineering and science that are too big to fit on available computers. Regardless of whether an analyst is using a personal microcomputer or a large supercomputer, the issue of available memory is an important one that often limits the type and scope of analysis that is to be performed. While increases in density of computer memory and efficient virtual memory management schemes have helped to alleviate the "supply" side of memory requirements, reduced coordinate methods (commonly termed "modal" methods) are an important means to help reduce the "demand" for more memory. These reduction schemes can be thought of as techniques to "make large problems small", while retaining as many of the important aspects of the solution's behavior as possible. Because a large problem is not small, reduced coordinate algorithms have the aura of "getting something for nothing", and so are an appealing area for study in computation. This report attempts to document some sample benefits and risks of using these modal analysis procedures in Civil Engineering applications.

The application of modal methods to large problems in Civil Engineering has a rich history. The classical technique of "normal-mode integration" from earthquake engineering is an example of a modal superposition method that has been used with great success on a wide variety of linear problems. Extensions of this approach to nonlinear problems are much more difficult from the dual standpoints of theory and application. Strictly speaking, the principle of superposition is not valid in a nonlinear environment, but appeals to local linearization of the underlying problem can be used to extend the mode superposition principle to this case. In a linear problem, one set of representative modes can be calculated at the outset, and used throughout the entire temporal analysis. Unfortunately, the effect of nonlinearities in a problem may be to turn an initially satisfactory set of modes into a poor estimate of the actual response of a system once substantial nonlinearities have developed. Development of robust schemes to update or augment a set of modes to account for solution nonlinearities is presently an important unanswered research issue that must be solved for the widespread use of nonlinear modal analysis to occur.

The theory and practice of modal analysis techniques are presented in Chapter 2 in the mathematical framework of projection methods. The example applications of Chapter 3 show the results of application of reduced coordinate schemes to a few representative problems in Civil Engineering. The final chapter reiterates the results of the applications, and suggests avenue for future research in this field.

Chapter 2

Review of Previous Work

Review of Previous Work

Modal projection methods have been used in a wide variety of solutions to problems in engineering, especially those involving structural dynamics and other time-dependent phenomena. The underlying theory for such projection schemes is developed in a previous report [1], as is a sample bibliography for this topic. Therefore, only the most important features of these methods will be presented here.

The Projection Theorem

The mathematical setting for projection solutions is a Hilbert Space, which is defined as a normed linear vector space, with the norm (length function for vectors) induced by an inner product. The most important interpretation of a Hilbert Space is that these abstract mathematical entities are the topological generalization of ordinary three-dimensional space. This means that such concepts as angle, perpendicularity, and completeness are preserved, even in an infinite-dimensional setting.

The fundamental properties of a Hilbert Space are defined in terms of the associated inner product of two vectors. The most important result for seeking approximate solutions to operator equations defined on a Hilbert Space is the Projection Theorem, which can be used to judge the quality of an approximation family. The geometric interpretation of the projection theorem for ordinary three-dimensional space is shown in Figure 1.

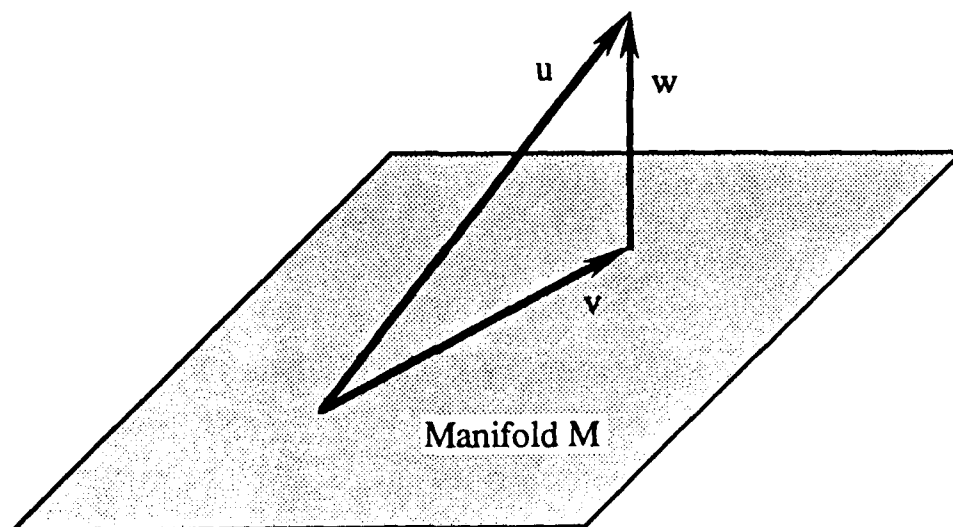


Figure 1: Geometric Interpretation of the Projection Theorem

Given a Hilbert Space H (in this case, R^3), and a complete manifold (subspace) M , the Projection Theorem states that every vector u in H can be uniquely decomposed into the sum $u = v + w$, where the vector v is in M and w is perpendicular to M . In the context of approximation, the manifold M represents a family of approximate solutions, and the vector $w = u - v$ represents the error in approximating u by any vector v in M . In this case, the Projection Theorem implies that the length of any error vector $w = u - v$ can be minimized by choosing w to be perpendicular to the approximation u , so that v , w , and u form an abstract generalization of a right triangle. The notions of length and perpendicularity depend on the underlying definition of the inner product that defines the Hilbert Space.

Two concrete examples of application of the Projection Theorem are:

1. Galerkin Finite Element approximations for self-adjoint boundary-value problems. In this case, the Hilbert Space is the space of all admissible solutions, and the inner product function is some type of associated potential energy functional for the boundary-value problem. The approximation manifold is the span of the Finite Element basis functions, and the error vector is the usual residual function. The familiar error-minimization interpretation of Galerkin's criterion for choosing the best approximate solution from the family is the minimum error vector length guaranteed by the Projection Theorem.
2. Reduced coordinate approximations for the Finite Element equations resulting from Example 1. In this setting, the underlying Hilbert Space is the finite-dimensional space of all nodal solution vectors, and the approximation manifold is the range of all matrices whose columns are the modes used for approximation. The inner product can be the "usual" dot product for vectors, or a weighted product induced by multiplication by the Finite Element mass or stiffness matrices.

In this setting, it appears that there is a distinct analogy between the following two questions:

- Q1. How many nodes (or basis functions) are required to obtain an acceptable solution quality for a Finite Element Model, and how should these nodes be chosen?
- Q2. How many modes are required to obtain an acceptable reduced coordinate approximation for a set of Finite Element equations, and how are these modes to be constructed?

Other standard concerns involving Finite Element approximation families (such as the use of mesh rezoning to update the solution family after permanent deformations have occurred) also have parallel interpretations in the setting of reduced coordinate models.

Eigenvector Expansion Methods

While the Projection Theorem can be used to choose the best approximation from a family of approximate solutions, the topic of the optimal choice (or construction) of this family is one not addressed directly by the Projection Theorem. Insight into this choice can be obtained by considering the spectrum of the operator that defines the problem to be solved.

The traditional approach to modal approximation for self-adjoint problems has been the use of exact eigenvectors as a reduced coordinate basis. The familiar "separation of variables" method for finding solutions to partial differential equations in terms of (truncated) Fourier Series is an example of the use of this approach, as is the "normal mode integration" procedure commonly used in dynamic structural analyses. Although there are alternatives to exact eigenvectors that are easier to construct, the use of eigenvector expansions is a useful theoretical tool for consideration of the choice of modes for a reduced coordinate analysis.

If the desired operator equation to be solved via a reduced coordinate method can be written in the general form $Ax = b$ (where A is a self-adjoint linear operator), then a consideration of the quality of various eigenvector projection schemes can be made by studying the set of eigenvalues of A . This set is known as the spectrum of A , and when A is a finite-dimensional operator (i.e., an $N \times N$ matrix), the spectrum consists of N real numbers (which are not necessarily distinct). For most stable structural systems, these real numbers are all positive, and in this case A is termed a coercive operator, or a positive-definite matrix. A picture of the spectrum of A for this situation is shown in Figure 2, where A 's eigenvalues are diagrammed in the complex plane.

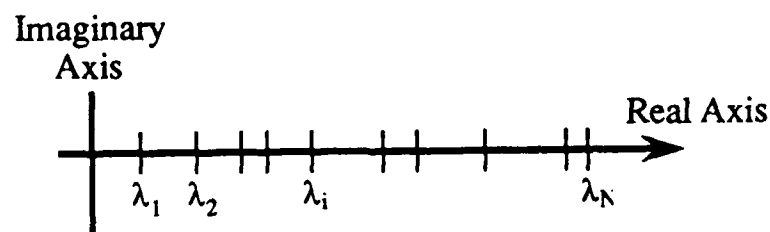


Figure 2: The Spectrum of a Positive-Definite Operator

For structural dynamics applications, the eigenvalues λ_i have the physical interpretation of squared frequencies, and so the minimal eigenvalues are associated with the lowest frequencies of vibration, and the maximal ones with higher frequency effects. When the frequencies of a discretized system (such as a Finite Element model of a structural system) are compared with the exact frequencies of the actual continuous system, it is generally true that the lower approximate frequencies are more accurate estimates for the true values than the higher frequencies. For example, the fundamental frequency for a Finite Element model of a structure is typically a very accurate estimate of the fundamental for the actual structure, but the agreement between higher frequencies may be very poor. Because of this phenomena, it appears that the use of eigenvector expansions for approximation purposes should begin with the lowest frequencies in order to achieve highest accuracy for a given number of modes.

Consideration of the expansion of the solution to $Ax = b$ in terms of A 's eigenvalues lends further credence to this approximation strategy. If the eigenvectors of A are denoted by u_i , then the solution x and the data b can be represented in terms of the eigenvectors by:

$$x = \sum_{i=1}^N \xi_i u_i \quad b = \sum_{i=1}^N \beta_i u_i$$

With this convention, the unknown coefficients ξ_i that define the solution x can be found by use of the defining relation for A 's eigenpairs:

$$Au_i = \lambda_i u_i \quad \text{implies that} \quad Ax = A \sum_{i=1}^N \xi_i u_i = b = \sum_{i=1}^N \lambda_i \xi_i u_i = \sum_{i=1}^N \beta_i u_i = b$$

Identification of each component in this equation gives a formula for the coefficients ξ_i :

$$\xi_i = \beta_i / \lambda_i$$

Thus the solution components are most sensitive to the smallest eigenvalues (the lowest frequencies), and the observation that the eigenvectors associated with the minimal frequencies will (in general) form the best approximation is verified. This is why the normal mode integration schemes are widely used for linear dynamics problems: the eigenpairs associated with the lowest frequencies lead to more efficient modal projection schemes.

Krylov Subspace Methods

Construction of exact eigenvectors involves finding an orthonormal set of vectors (i.e., a new coordinate system) that diagonalizes the operator A , so that the coupled operator equation set resolves into uncoupled scalar forms when referred to this new coordinate system. Other "distinguished orthonormal sets" exist that allow the operator A to take special simple forms, and these alternative coordinate systems may be considerably easier to construct than a set of exact eigenvectors. Probably the most important of these orthonormal sets is that generated by the Krylov Sequence:

$$Ay, A^2y, A^3y, A^4y, \dots$$

The manifold spanned by vectors from this sequence is termed the Krylov Subspace $K(A, y, m)$

$$K(A, y, m) = \text{span} (Ay, A^2y, A^3y, \dots, A^my)$$

It can be shown [Reference 10] that for self-adjoint A , the vectors of the Krylov Sequence form a three-term recurrence, so that A is tridiagonal when referred to an orthonormal basis for $K(A, y, m)$. This fact forms the basis for the Lanczos Algorithm, which constructs this basis in a computationally efficient manner.

Since a tridiagonal form of the operator A is not appreciably more difficult to use than a diagonal one, there is a strong incentive to use the Krylov Subspace, since construction of this manifold is considerably simpler than construction of an equal number of exact eigenvectors.

It is easy to show that successive vectors in the Krylov Sequence tend towards the eigenvectors associated with the maximal eigenvalues by considering the expansion of the initial vector y in terms of the eigenvectors of A .

If $y = \sum_{i=1}^N \xi_i u_i$, then the Krylov sequence $Ay, A^2y, A^3y, \dots, A^my$ can be written as:

$$\sum_{i=1}^N \lambda_i \xi_i u_i, \quad \sum_{i=1}^N \lambda_i^2 \xi_i u_i, \quad \sum_{i=1}^N \lambda_i^3 \xi_i u_i, \quad \dots, \quad \sum_{i=1}^N \lambda_i^m \xi_i u_i$$

As m increases, the terms involving λ_N , λ_{N-1} , λ_{N-2} , ... dominate, since these eigenvalues are the largest in magnitude. This leads to the following convention (which is not standard, but will be used in this document):

A Forward Krylov method for approximating the solution of $Ax = b$ is one that uses the Krylov Subspace $K(A, y, m)$ associated with the operator A as an approximate solution manifold.

A Backward (or Inverse) Krylov method is one that uses the Krylov Subspace $K(A^{-1}, z, m)$ associated with the inverse of A as an approximate solution manifold.

Since the eigenvalues of A^{-1} are the reciprocals of those for A , a backward Krylov scheme uses information from the eigenpairs at the low-frequency end of the spectrum, and a forward scheme uses data from the high-frequency end of the spectrum. It is apparent from the discussion above that the backward schemes are typically more efficient in terms of number of modes required to form an approximate solution, but the issue of expense of forming each mode should also be considered. Each vector added to the forward sequence requires a matrix multiplication by A , compared to the solution of a set of equations involving the coefficient matrix A required for each vector in the backward sequence. Thus each vector in a backward scheme requires considerably more work to form, which reduces the efficiency of the method. In addition, if A is singular (or nearly so), the solution of the system $Ay_i = y_{i-1}$ to obtain the next vector in the sequence may not be feasible. This would be the case if the structural system of interest possessed some type of instability (another source of near-singularity will be presented in the next chapter).

Based on this elementary analysis of Krylov Subspace methods (i.e., "all other things being equal"), the following general characteristics of the two strategies can be contrasted:

Forward schemes will require more vectors to achieve a given accuracy of approximate solution, but each vector in the spanning sequence will be easier to form. The approximate solution manifold will be dominated by information from the high-frequency end of the spectrum, which is less desirable from the standpoint of accuracy, but zero eigenvalues (corresponding to structural instability) should cause little problem for this family of methods.

Backward schemes will require fewer vectors for given accuracy, but each vector will be more difficult to form. The solution manifold will be dominated by low-frequency data (which is desirable for accuracy), but the effects of zero eigenvalues must be alleviated.

Examples of forward Krylov projection schemes include the Conjugate-Gradient Method (CGM) [3,8], and the Lanczos Algorithm [1,2,9,12,13,14,15]. In a nonlinear time-dependent problem, these schemes involve reconstructing an appropriate Krylov Subspace at each solution step (i.e. for each equation of the form $A(x,t) x(t) = b(x,t)$ that is to be solved). This reconstruction is feasible only because each vector in the sequence is easy to form via a matrix multiplication, and has the advantage that the approximation subspace "tracks" the evolution of the operator $A(x,t)$ through the effects of both time and solution nonlinearities. The biggest disadvantage of these schemes is that when A is ill-conditioned (i.e., the range of scales of the frequencies is large), these methods may converge very slowly, or not at all. This difficulty can often be ameliorated by compressing the spectrum by premultiplication of $Ax = b$ by an operator chosen to improve the condition of A . Such a matrix is termed a preconditioner, and the efficient construction and application of preconditioners forms the basis for virtually all of the practical Conjugate Gradient schemes [8,11].

An example of a backward Krylov method is the Inverse Lanczos Algorithm, which is used in the next chapter to find approximate solutions of some representative engineering problems. This approach is the generalization of "normal mode integration" techniques to Krylov approximations for nonlinear problems. The details of this method have been elucidated in a previous report [10].

Chapter 3

Example Applications

Example Applications

This section illustrates the application of modal coordinate methods to some representative problems in Civil Engineering. The three problems considered illustrate a range of solution behaviors, as well as different amounts of success that can be encountered when a reduced coordinate analysis is used. The first problem involves a dynamic (blast) problem, while the second is a time-dependent model that is diffusive in character. The final problem is an example of how a "backward" reduced coordinate scheme can encounter difficulties in certain settings.

Bounding-Surface Soil Dynamics

The first application considered involves the dynamic response of a building founded in relatively soft soil. The building is loaded by a blast for a duration of two seconds. The blast pressure starts at zero, and grows linearly for those two seconds, reaching a maximum of four psi. For all time after the initial two-second blast, the pressure is taken as zero. Thus, the applied load acts for only the initial two seconds, and the soil-structure system responds in free-vibration afterward.

The geometry of the problem is shown in Figure 3, and the appropriate boundary conditions are illustrated in Figure 4 (this figure also shows the location of two particular elements that are used to monitor the behavior of the analysis). The building is modelled as an isotropic, linear-elastic continuum in plane strain, which is appropriate for a "shear-wall" building (where infilling panels contribute significantly to the strength of the building's lateral-force resisting system). The material properties for the building are given by:

$$E_{\text{bldg}} = 1.0 \times 10^7 \text{ psf}$$

$$\nu_{\text{bldg}} = 0.18$$

$$\gamma_{\text{bldg}} = 75 \text{ pcf}$$

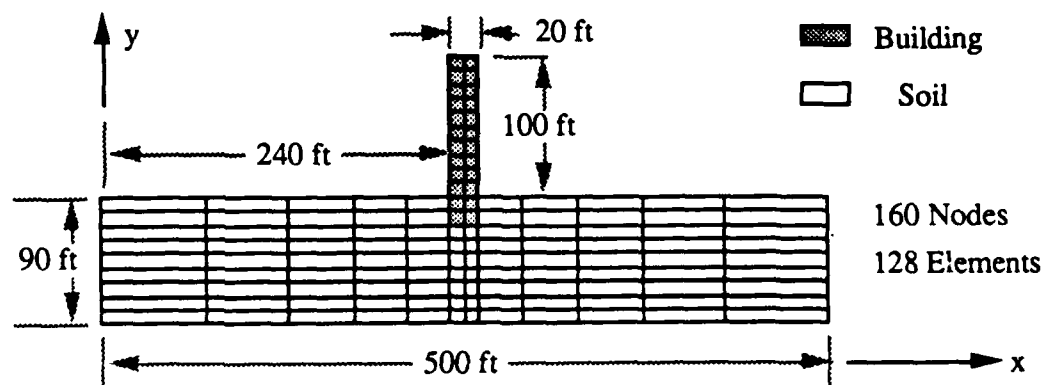


Figure 3: Geometry for the Soil Dynamics Problem

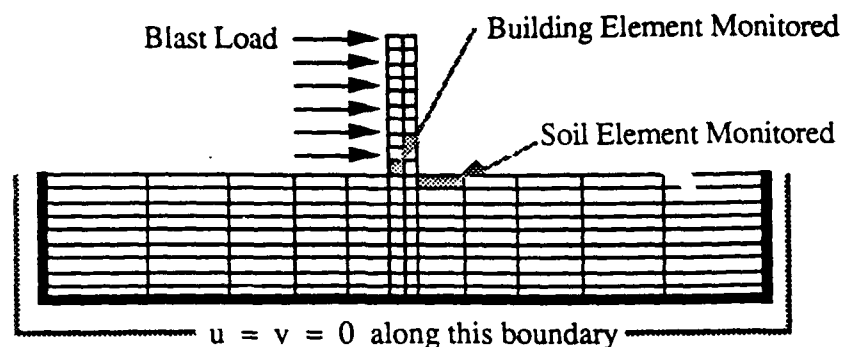


Figure 4: Boundary Conditions for the Soil Dynamics Problem

The soil material is characterized using bounding-surface plasticity for clays [4,5,6,7], and the material parameters for the soil are given in Figure 5. The clay soil is idealized as slightly overconsolidated, with an excess pressure equal to 1250 psf (i.e., as if the soil deposit had been consolidated sometime in the past under an additional 10 foot overburden with the same unit weight).

$v_{\text{soil}} = 0.2$	$\gamma_{\text{soil}} = 125 \text{ pcf}$	$\lambda = 0.075$	$\kappa = 0.010$
$P_1 = 6.35 \text{ psf}$	$P_{\text{atm}} = 2117 \text{ psf}$	$M_c = 1.350$	$M_e/M_c = 2/3$
$R_c = 3.050$	$R_e/R_c = 0.560$	$A_c = 0.175$	$A_e/A_c = 0.850$
$T = 0.010$	$C = 0.485$	$S = 1.000$	$m = 0.020$
$H_2 = 1.900$	$H_c = 2.000$	$H_e/H_c = 0.875$	

Figure 5: Clay Material Parameters

The initial state of the clay under the building's load was obtained by solving the quasistatic problem of the soil-structure system loaded by its own weight. The resulting soil pressures were used as the initial stress state for the elements in the clay layer.

The analysis of the building was carried out using the Newmark-Newton method of [10]. The temporal discretization involved 100 time steps, each of length 0.1 second. The use of a longer time step resulted in more "sub-stepping" by the temporal integration scheme, which led to greater computational cost. Both the direct (unreduced) formulation and the reduced coordinate approach used incremental displacements as primary unknowns, since the bounding surface plasticity model

involves an incremental stress-strain relation. In the reduced formulation, results were obtained for 2, 4, and 8 Lanczos vectors. In each case, these vectors were generated with the spatial distribution of the blast load used as the starting vector for the Krylov Sequence. This choice corresponds to choosing the initial mode to correspond to a pseudo-static response to the applied blast force. Adding vectors beyond a four-dimensional subspace did not appreciably increase the accuracy of the analysis, but began to increase the computational effort. In this problem, the reduced algorithm typically used approximately one-third as much computer time as did the unreduced problem (even though the code used for the reduced algorithm is heavily instrumented in order to develop and evaluate the projection solution scheme, while the program for the direct formulation is a much more efficient "production" code). Because of this fact, and also because this problem is still relatively small in terms of the size of the equation set, the computational advantage of the reduced algorithm is somewhat conservative. It is expected that the reduced scheme will give even greater efficiencies on larger problems, especially those resulting from three-dimensional models.

The shapes of the displacement fields for the first four Lanczos vectors ("modes") are shown in Figure 6. These patterns of displacement are magnified a thousand times because the normalization of these modes with respect to the mass matrix yields actual displacement components that are on the order of thousandths of a foot. As may be noticed in Figure 6, the shape of the displaced building in the first mode appears to incorporate some rigid rotation of the building under the applied load, and the next two modes clearly demonstrate bending behavior of the building.

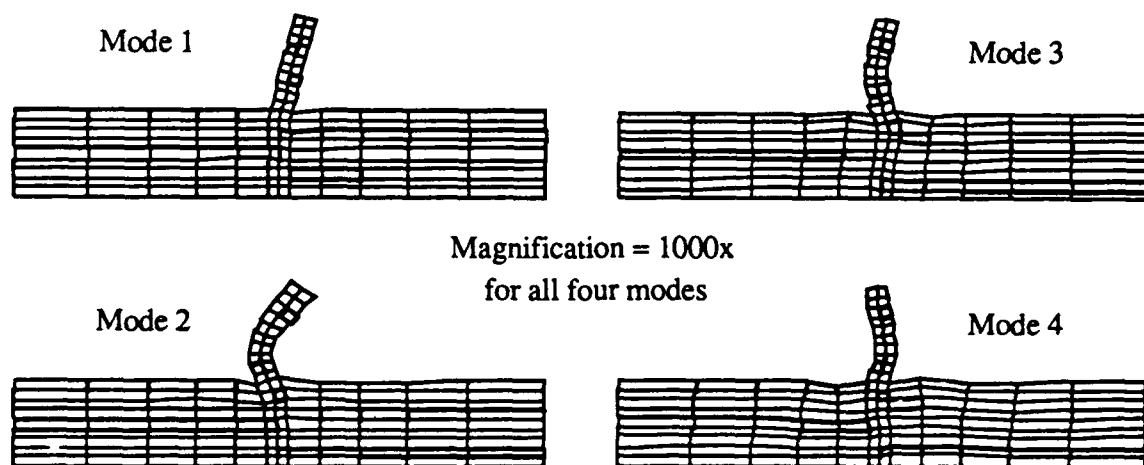


Figure 6: Lanczos Modes for the Soil Dynamics Problem

Some representative results of the analyses are shown in Figures 7 through 11. In Figures 7 and 8, the horizontal displacements at the bottom and top of the building are plotted as functions of time. It is clear from these graphs that the reduced coordinate analyses are producing reasonable approximations to the overall behavior of the mechanical system, but that the direct scheme predicts the permanent set of the building (and the associated residual stresses in the clay) much more accurately. This is because the modal analyses involve projection vectors that do not include large plastic effects, and thus cannot accurately represent the permanent strains due to the blast loading. In addition, the reduced analyses underestimate the amount of energy dissipation of the nonlinear material model. In fact, if the nonlinear convergence tolerance is relaxed for the reduced algorithm, the response approaches that of a linear problem, with little or no losses due to plasticity.

It is apparent from these results that problems governed by inelastic effects will require special attention from any successful modal analysis scheme. In particular, some means of either updating the modes to include plastic deformation, or of increasing the size of the projection subspace will be required for high accuracy from this family of approximate solution techniques. Given the very slight increase in accuracy observed in this problem when the number of modes is increased, it appears that modal updating schemes are the most appropriate path for future work in this area.

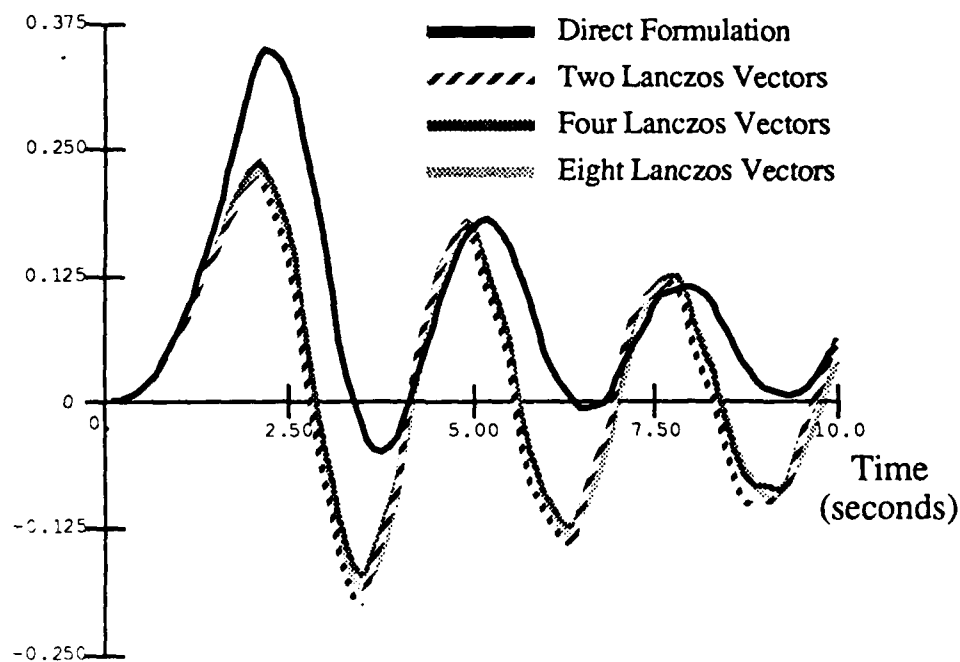


Figure 7: Horizontal Displacements at the Bottom of the Building

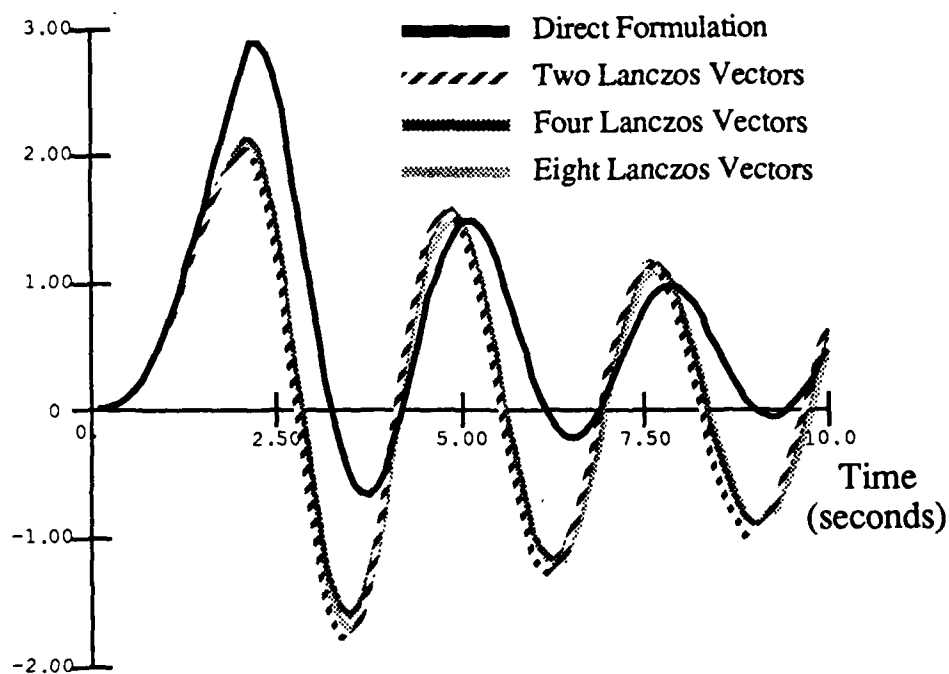


Figure 8: Horizontal Displacements at the Top of the Building

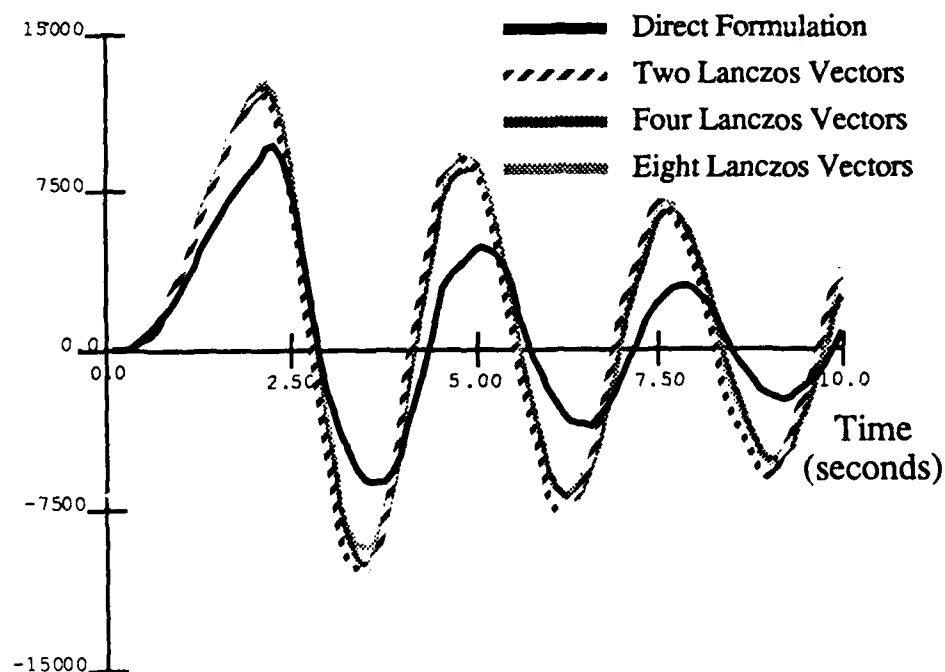


Figure 9: Bending Stresses at the Bottom of the Building

Figures 9, 10, and 11 depict representative building and soil stresses for the elements highlighted in Figure 4. These stresses show better agreement between direct and reduced results than the displacements displayed in Figures 7 and 8. As in the comparison of displacements, the addition of more modes did not produce significantly better results, which reinforces the view that some means of updating a small number of modes is probably a more efficient reduced coordinate strategy than increasing the size of the projection subspace.

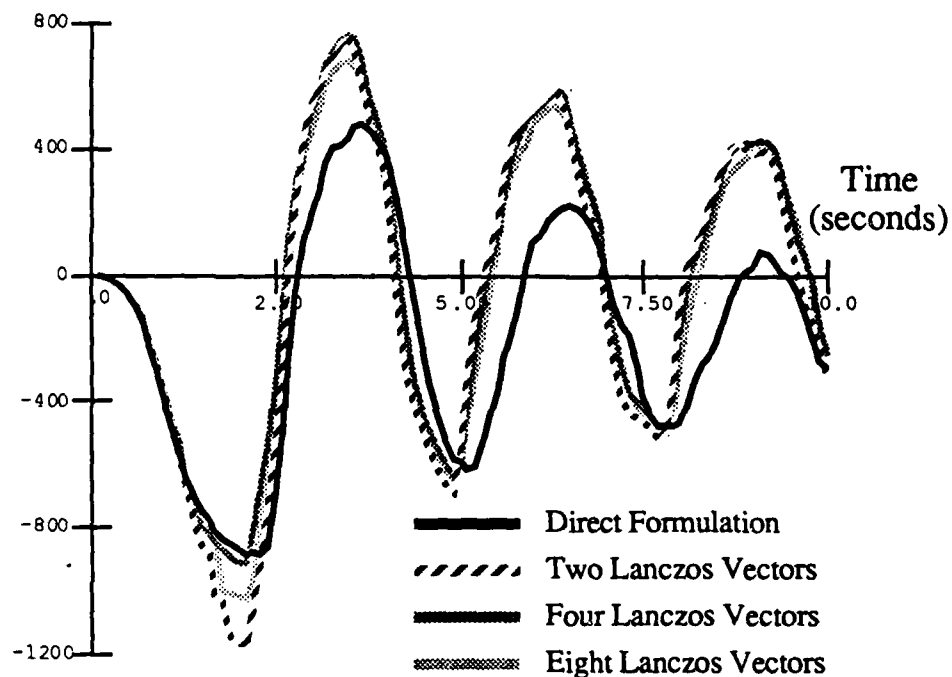


Figure 10: Axial Soil Stresses at Base of Building

This example demonstrates that the reduced scheme can be used to obtain reasonable approximations to difficult problems in dynamics, and that such reduced coordinate algorithms warrant further study. Even with the present underestimation of the plastic effects in this problem, the reduced approach is useful as a less expensive tool for a preliminary analysis. In addition, its memory requirements are extremely small compared to the direct method, since the global stiffness, tangent stiffness, and mass matrices do not need to be formed, stored, or factored. The next example problem demonstrates a nonlinear time-dependent problem where these memory needs are very important.

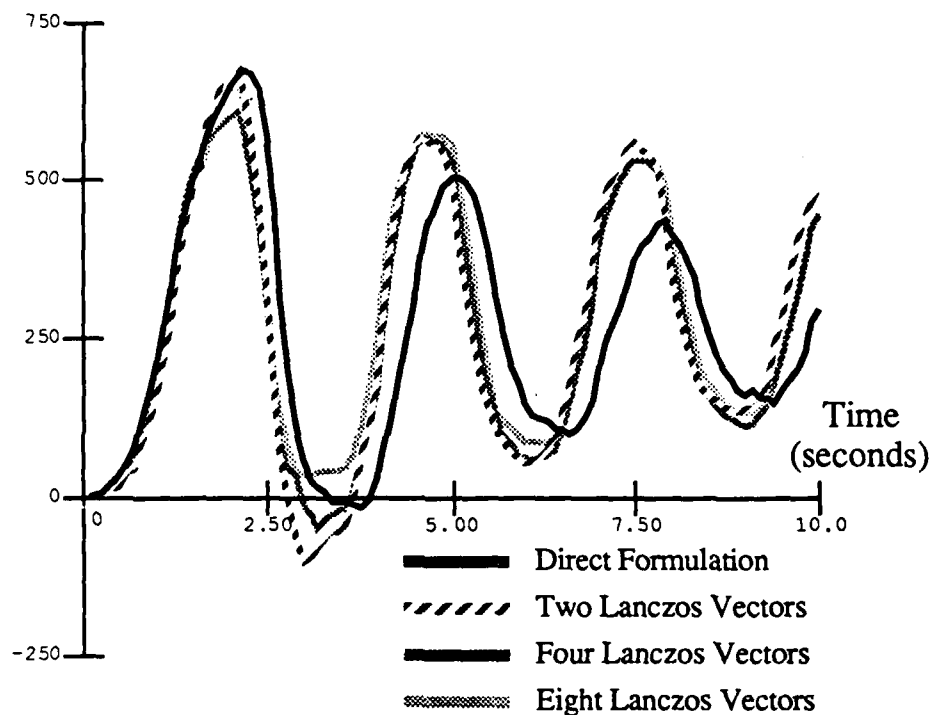


Figure 11: Soil Shear Stresses at Base of Building

Nonlinear Flow in a Porous Media

Another important time-dependent phenomena involving soils involves the flow of fluids through soil voids. Examples of this problem are soil consolidation (where the fluid is porewater), gas migration (where the fluid is air or methane), and contaminant transport (where a contaminating fluid is carried through the soil voids by the motion of groundwater). All of these are important "real-world" problems of considerable interest to engineers, and all can be approached from a reduced coordinate standpoint. Methods for practical solution of soil consolidation problems have been addressed in [7], and contaminant transport problems are governed by a non-self-adjoint boundary-value problem that is an object of present research by the authors (recall that much of the theoretical framework presented in the last chapter involved self-adjoint problems). The problem of gas migration through soils is governed by a generalization of the familiar diffusion equation, and is a good candidate for a reduced coordinate formulation.

In this case, the fluid is methane gas produced by the decomposition of solid waste in a municipal landfill, and the porous medium includes both soil and the waste itself, but the basic principles and solution process for this problem are readily applicable to many other problems involving diffusive phenomena. In the setting of gas production, this model can be taken as a "zeroth" order approximation to a very complicated problem that is of urgent importance in many urban areas. Many of the simplifications made are somewhat crude, but they serve as a good starting point for a more refined physical and mathematical analysis. The primary interest in this problem from the standpoint of this reduced coordinate research is that the gas model produces an interesting nonlinear problem, and the reduced scheme promises to allow reasonable approximate solutions to be found using microcomputers such as those that can be found in many small engineering firms.

The governing equation for two-dimensional flow in a porous medium is given by the diffusion equation:

$$c \frac{\partial u}{\partial t} - \left\{ \frac{\partial}{\partial x} \left(k_x \frac{\partial u}{\partial x} \right) + \frac{\partial}{\partial y} \left(k_y \frac{\partial u}{\partial y} \right) \right\} + bu = f$$

The functions c , k_x , k_y , and b are material parameters, $u(x,y)$ is the solution (pressure, in this case), and f is a source term, which can include singular behavior such as point sources. The coefficient c represents the "storage" capacity of the medium, the functions k_x and k_y represent the medium's ability to conduct fluid, and the term b reflects the convection of fluid in the direction perpendicular to the plane (i.e., leakage to the atmosphere). This equation is a first-order differential equation in time, and similar equations govern a wide variety of diffusive problems.

In the context of the gas production problem, the source function f depends on time, since the bacterial decomposition process that produces the gas is dependent on temperature and water supply, both of which may vary with the season. In addition, because there is a period of time between the placement of the landfill and the onset and development of microbial decomposition, the time dependence of the source term is modelled by separating this term into two parts:

$$f(x,y,t) = h(t) s(x,y)$$

The function $h(t)$ represents a "history" function whose long-range average is unity, and this function scales the spatial source term $s(x,y)$. The history function $h(t)$ used in this example problem is shown in Figure 12.

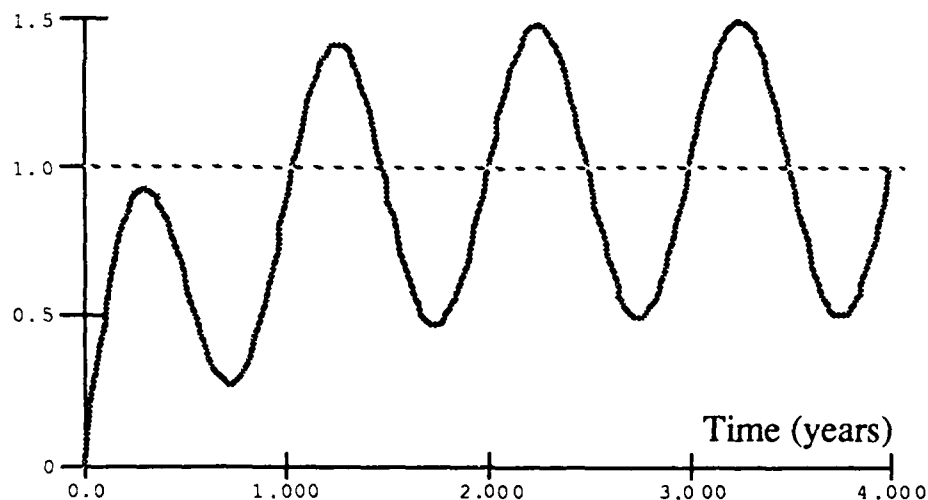


Figure 12: History Function for Gas Production

The domain of the problem is actually three-dimensional, but a horizontal plane in the landfill is modelled as a simple two-dimensional approximation. It is assumed that the soil cover above the landfill allows some migration of the gas in a direction perpendicular to the plane, and that this migration is dependent on the pressure in the landfill, since large enough pressures should allow the gas to breach the soil cover. In this problem, this variation in perpendicular permeability of the cover is modelled using a nonlinear convection function $b = b(x, y, u)$ defined by:

$$b(x,y,u) = b_0(x,y) + \beta(x,y) u^2$$

This quadratic convection coefficient represents a soil cover that "heals" after being subjected to large pressures. Many other choices are possible, and the most appropriate representation for this term is still under study. The material parameters used for the model are tabulated in Figure 13, and the two dimensional domain is shown in Figure 14.

$c = 1$	$k_x \approx 1$	$k_y = 1$
$b_0 = 1$	$\beta = 1$	$s(x,y) = 10$

Figure 13: Material Properties for the Gas Model

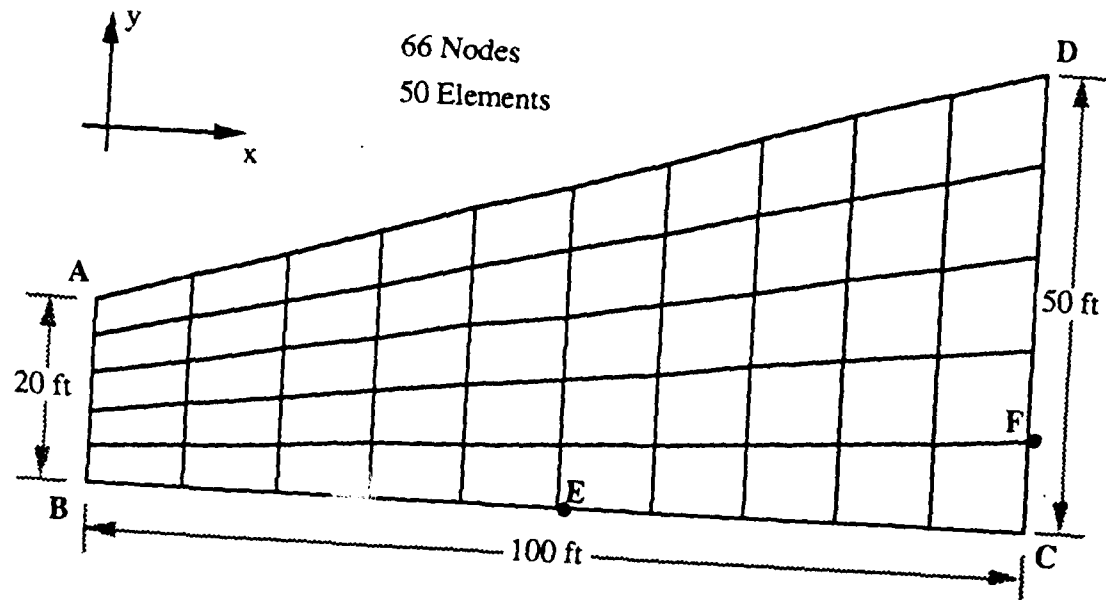


Figure 14: Solution Geometry for the Gas Model

The boundary conditions used for this example problem involve the labelled points in the mesh of Figure 14. A condition of zero pressure is maintained along line segment AB, and the pressure is also required to vanish at the node labelled C. This latter condition corresponds to a test well placed in the fill to relieve pressure. All the rest of the boundary satisfies a zero normal flow condition (i.e. an insulated boundary). The two nodes labelled E and F are points where the solution history for the various analyses will be compared.

It should be reiterated that this solution process is only a simple approximation to a very important complex problem. The large number of "ones" in Figure 13 reflect a choice of parameters that is not intended to model a particular site, but only to serve as a starting point for a more involved analysis of this problem. In this same vein, the units used in the analysis do not reflect any particular conventions, except the desire to work with units that are reasonably close to those expected in the field.

Application of a Finite Element discretization process to the spatial terms in the diffusion equation leads to the following system of ODE:

$$Mv + Kp = f$$

where $\dot{v} = \partial p / \partial t$ is the time rate of change of the vector p of nodal pressures. Formulae for the mass M and stiffness K can be found in any standard Finite Element text, though it should be noted that the stiffness K depends on p , so this problem is governed by a nonlinear system.

The required temporal integration scheme can be developed by expressing the pressure p at time t_{n+1} in terms of the "velocity" \dot{v} at t_{n+1} and terms evaluated at time t_n :

$$p_{n+1} = p_n + (1 - \alpha)\dot{v}_n h + \alpha\dot{v}_{n+1} h \quad (h = t_{n+1} - t_n)$$

This relation for p_{n+1} in terms of \dot{v}_{n+1} can be inverted to cast the pressure p as the primary independent variable:

$$\dot{v}_{n+1} = \frac{1}{\alpha h} (p_{n+1} - p_n) - \frac{(1 - \alpha)}{\alpha} \dot{v}_n$$

A "predictor" step can be formed by using this result to write the governing matrix equation at the end of the time step ($t = t_{n+1}$) entirely in terms of the pressure vector:

$$K_{eff} p_{n+1} = f_{eff}$$

$$\text{where } K_{eff} = K + \frac{1}{\alpha h} M$$

$$f_{eff} = f_{n+1} + M \left[\frac{1}{\alpha h} p_n + \frac{(1 - \alpha)}{\alpha} \dot{v}_n \right]$$

A Newton "corrector" scheme can be derived in this case (where M and f are not functions of the pressure p) by defining a residual vector r :

$$r(p) = K(p) p + M \dot{v} - f(p) p$$

The (vector) zeros of this residual can be found by solving the relation:

$$r'((i-1)p) [(i)p - (i-1)p] = -r((i-1)p)$$

$$\begin{aligned} \text{with } r'(p) &= \left[\frac{\partial K}{\partial p} p + K \right] + M \frac{\partial \dot{v}}{\partial p} - \frac{\partial f}{\partial p} \\ &= \left[\frac{\partial K}{\partial p} p + K \right] + \frac{1}{\alpha h} M - \frac{\partial f}{\partial p} \end{aligned}$$

(where i is the iteration counter) until convergence to a fixed point is obtained. In the gas-production problem, the quadratic nonlinearity in $b(x,y)$ leads to a symmetric tangent stiffness $[(\partial K/\partial p)p + K]$. More complicated nonlinearities (e.g., those affecting the conductivity terms) may lead to a non-symmetric tangent stiffness.

This "predictor-corrector" algorithm was used to solve the gas-production problem for three cases:

- (1) A direct formulation involving the mesh of Figure 14
- (2) A direct formulation for a refined mesh obtained by subdividing each element from analysis (1) into four elements.
- (3) Reduced solutions involving 1 to 4 Lanczos vectors and the coarse mesh of analysis (1).

The four Lanczos vectors ("modes") used in analysis (3) are shown in Figure 15.

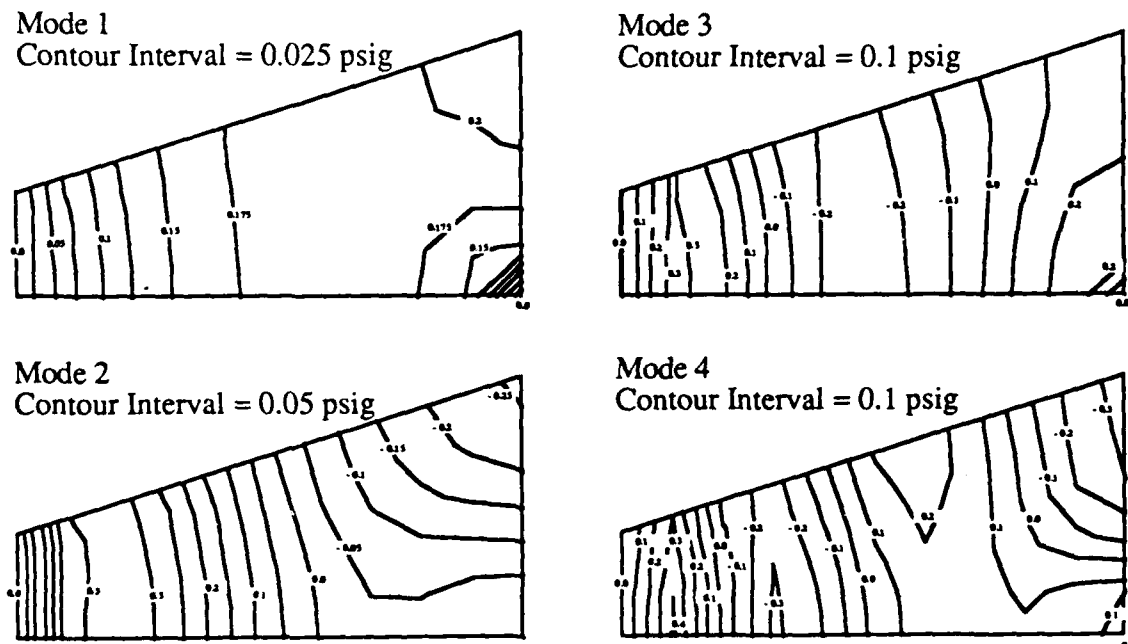


Figure 15: Lanczos Modes for Gas Flow Problem

Results from the various analyses are shown in Figures 16, 17, and 18. Plots of pressure against time are found in Figures 16 and 17 for the two sampling points E and F shown on Figure 13. The "exact" solution (black line) is the curve for the coarse mesh — results for this mesh are practically identical to those from the refined mesh, leading to the conclusion that this solution has essentially converged. The modal analyses that are not shown coincide with this "exact" solution

and are not plotted. Figure 18 shows the distribution of pressure at the end of the analyses. The modal results are excellent approximations to the "exact" solution even after 60 time steps (3 years).

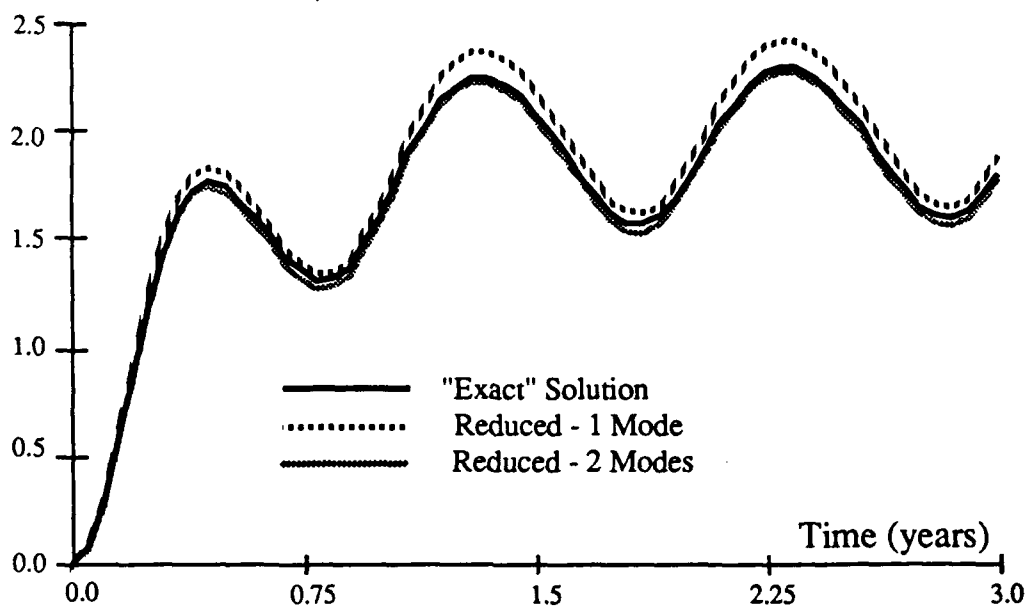


Figure 16: Solution History for Well "E"

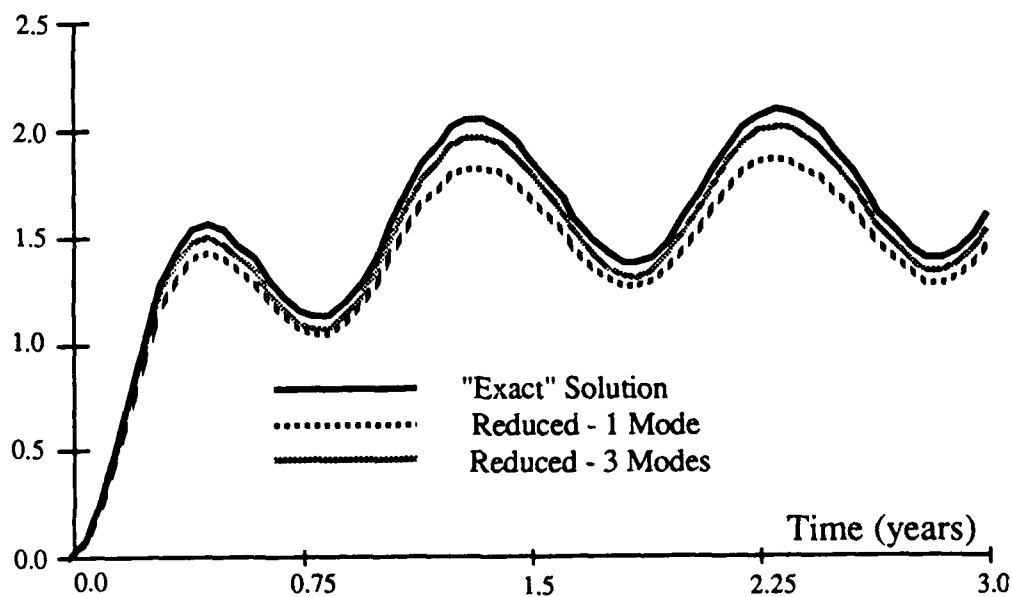


Figure 17: Solution History for Well "F"

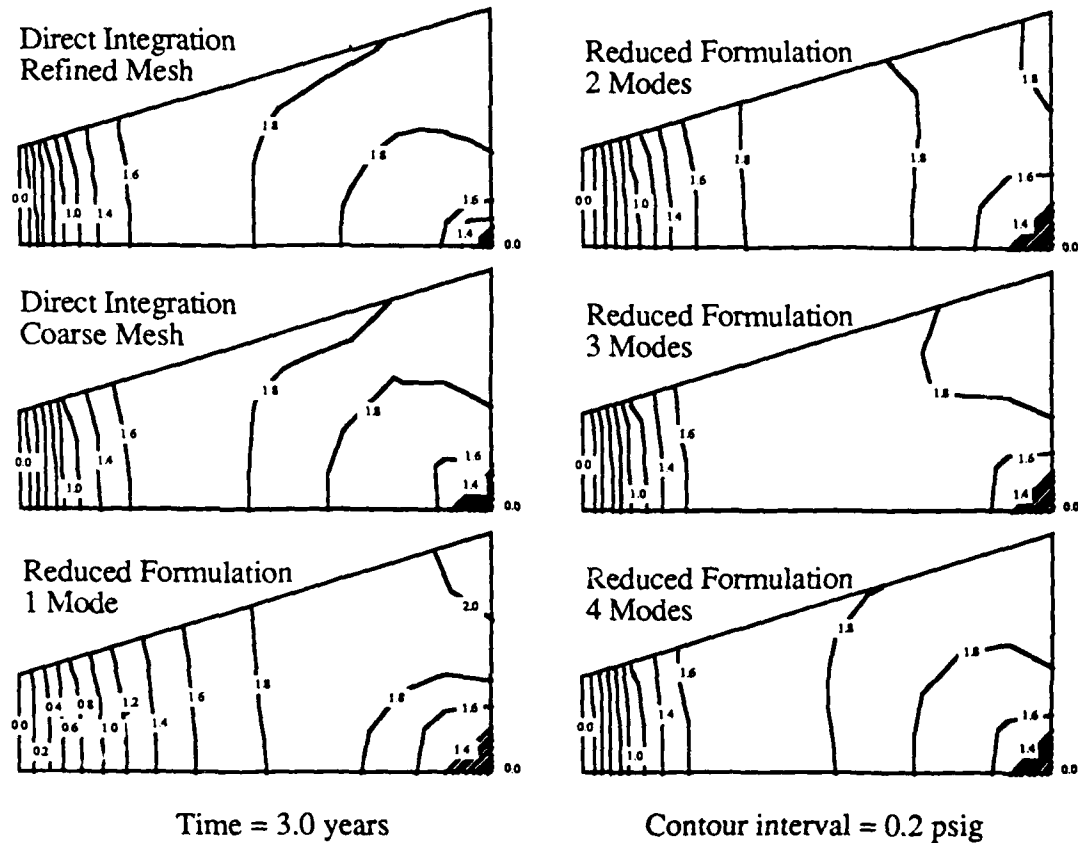


Figure 18: Final Solution Contours for Gas Flow Problem

This example is clearly a successful application of a reduced coordinate method to an important problem in Civil Engineering. The solution efficiencies encountered here promise that three-dimensional problems of this type should be solvable even on low-cost microcomputers. The actual behavior of this solution depends almost entirely on the "low-frequency" modes (recall that there are no dynamic effects here), and the original mode shapes capture the solution behavior even after substantial nonlinearities have developed. This is a typical result for a problem for a self-adjoint (in the linear case) problem where the data primarily excites the lowest frequencies. The next example, however, demonstrates that this excellent agreement between reduced coordinate approximation and direct formulation is not always observed.

Soil Dynamics Incorporating Porewater Effects

The response of soils of low permeability (such as clays and fine silts) to dynamic loads is largely governed by the rate at which porewater trapped in the soil voids can flow. The soil-water system thus acts like a large sponge in that the deformations of the solid phase are influenced by the rate at which the fluid phase responds to changes in pressure. Thus any completely realistic model of structural behavior for cohesive soils will have to consider the effects of pore pressure. One of the most important of these effects is that a relatively impermeable soil behaves as a nearly incompressible medium, which often necessitates using low-order (reduced) integration on various volumetric energy terms in order to prevent the Finite Element solution from "locking-up" (i.e., seriously underestimating the magnitude of displacements).

For the problem of soil consolidation, the structural response of the soil mass is quasistatic, and inertial effects can be neglected. This class of time-dependent problems is developed in [7], where a Finite Element analysis for consolidation of clay soils is presented. The soil dynamics model used in this third and last example uses the basic equations of this Finite Element soil code, with *inertial terms added to account for dynamic effects*. The behavior of porewater is modelled by inclusion of additional displacements at each node, which represent the movement of the porewater relative to the soil skeleton. A detailed derivation of this entirely displacement-based formulation of the soil dynamics problem can be found in [17]. In this reference, it is mentioned that the formulation may suffer from "hourglassing", which is an oscillatory phenomenon that erodes the quality of the solution. This hourglassing response arises from the introduction of spurious low-energy deformation modes produced as an unwanted by-product of the low-order integration terms. Technically, these hourglassing effects are termed spurious singular modes, because they are unwanted (and incorrect) solution "shapes" that correspond to near-zero eigenvalues of the Finite Element equation set.

The effect of these singular modes is shown in Figure 19, which is a plot of two Lanczos vectors obtained from a backward modal projection scheme (compare with Figure 6). The problem that is modelled is the same as the first example problem of this chapter, but generalized in the manner of the last paragraph to include porewater flow. The direct (unreduced) solution gives reasonable results (which are similar to those of Figures 7 through 11), but the results of the reduced coordinate formulation for this case are completely incorrect, and underestimate the solution displacements by several orders of magnitude. The two Lanczos vectors shown give the reason for this complete degradation of solution quality: the dynamic response of the soil-building

structure does not even appear in these modes used for the reduced solution, so that the reduced coordinates cannot account for any movement of the structural system. The problem is that the spurious hourglassing shapes appear in the problem as extremely low-frequency vibrational modes, which are then detected and used by the backward projection scheme to the exclusion of the correct (i.e., non-spurious) modes. The ability of backward projection methods to identify the low-frequency response of a structural system has been obviated by the fact that the lowest frequencies of this Finite Element model are entirely spurious!

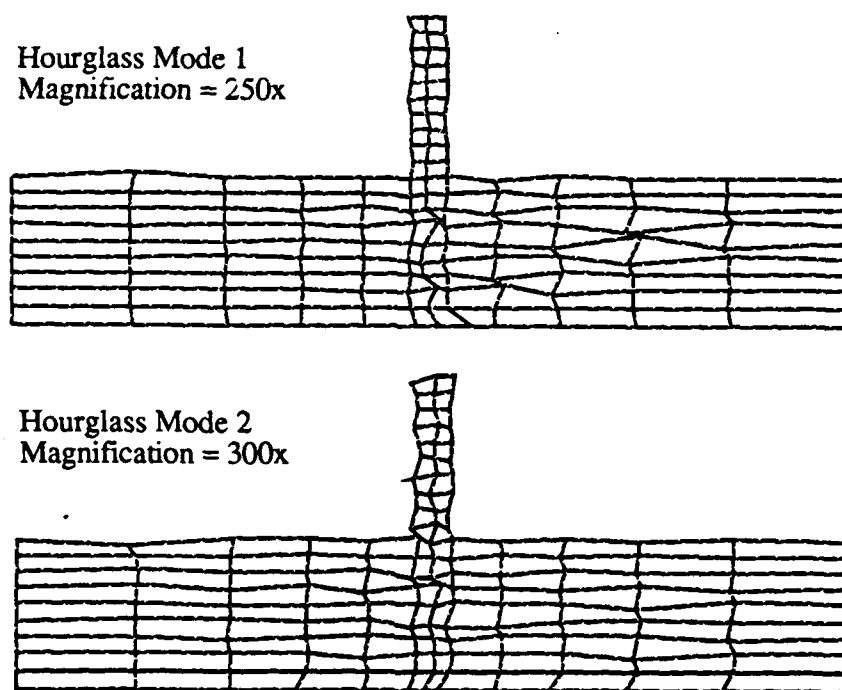


Figure 19: Sample Hourglass Modes for Soil Dynamics Problem

This result could have been predicted by the analysis of Chapter 2, where it was shown that a structural system possessing near-instabilities would cause difficulties for a backward projection method. This problem (in its present form) would be better solved by a forward projection scheme such as a preconditioned forward Lanczos method, which would converge from the high-frequency end of the spectrum and thus avoid the spurious hourglassing modes.

A better approach would involve not using models with pathological behavior such as these singular modes. The problem with hourglassing can be removed by using a mathematically more correct mixed formulation and a better choice of element interpolants, or by adding fictitious viscosity to the model for the purpose of "hourglass control". This example is intended to show that "backward" reduced coordinate methods cannot be blindly applied to arbitrary types of Finite Element problems, but only to those cases where the solution is primarily dependent on a relatively small number of lower-frequency modes of response.

These examples demonstrate the notion that reduced coordinate models are a useful tool for cutting many large intractable problems down to a more manageable size, but this approach should be used with caution where pathological problems with the formulation are known to exist. Modal analysis procedures are thus one more computational tool for solving large problems, but should not be viewed as a panacea for curing all the difficult problems in computational mechanics.

Chapter 4

Extensions

Extensions

Suggestions for Further Study

The reduced coordinate scheme introduced in [10] and applied in this document can be seen to be a useful solution tool for many types of engineering problems, but there is clearly more work that is needed to make this technique more reliable, robust, and efficient. A few of the areas where future development and/or application is warranted include:

- (1) Application of the method to framed structures. These systems are typically very dependent upon low-frequency response, and are thus likely candidates for efficient application of the proposed reduced coordinate scheme. Present research by the authors involves application of these modal methods to two- and three-dimensional frames which incorporate nonlinear material effects through the use of bounding-surface plasticity models relating moment and curvature. Preliminary efforts in this area have demonstrated that the reduced coordinate model is an appropriate tool to reduce the size of problems of this class.
- (2) Application of the method to soil dynamics problems involving porewater effects. Although the naive implementation of the reduced coordinate model for the last problem of the preceding chapter showed poor results, it appears that this method can be useful in this case, as long as it is applied to a formulation that does not exhibit spurious singular modes. Attention is being focused on mixed Finite Element models that satisfy consistency conditions on displacement and pressure interpolants designed to inhibit the existence of these spurious modes. In addition, generalization of the theoretical framework of the projection scheme to accommodate non-self-adjoint problems (such as those arising from bounding-surface characterizations for sands) is an object of continuing research.
- (3) Development of schemes for updating modes to account for inelastic effects. This research is proceeding for both *continuum* and framed structures, and is concentrated on efficient modal update schemes that do not result in any truncation errors from the change in projection basis. Since the Finite Element method itself is a projection method, one promising avenue of research is to view the modal update procedure as an analog of a Finite Element mesh rezoning problem (where many proposed schemes have been developed). Mapping the solution from one modal basis to another without truncation error may be affected in a manner similar to a mesh remapping algorithm. This topic is the subject of continuing research by the authors.

Conclusions

The reduced coordinate schemes applied in this report show considerable potential to solve a variety of important engineering problems. Placed in the context of projection methods, they can be seen as part of a unified array of methods that includes the Conjugate Gradient Method, the Lanczos Algorithm, and modal superposition schemes. All of these approaches share the common characteristic that each may be used to make certain large intractable problems solvable on a variety of computers, and thus extend the range of problems that can be solved. The examples presented demonstrated a spectrum of success in the application of the backward modal analysis schemes ranging from excellent agreement to near-total failure. On non-pathological problems typical of those encountered in practice, the reduced scheme performed well in that essential phenomena were captured while decreases in computer expense were observed. On the "ill-behaved" problem presented, the modal scheme gave poor results, but the source of the difficulty was seen to be a shortcoming in the formulation of the unreduced model, and the poor results could be alleviated by a more appropriate choice of projection scheme.

In summary, the reduced coordinate method has demonstrated its utility on a number of important problem in Civil Engineering, and warrants further work to extend the range of its usefulness.

References

1. Bayo, E.P., and E.L. Wilson, 1984a, Use of Ritz Vectors in Wave Propagation and Foundation Response, *Earthquake Engineering and Structural Dynamics*, Vol. 12, Pg. 499-505
2. Bayo, E.P., and E.L. Wilson, 1984b, Finite Element and Ritz Vector Techniques for the Solution to Three-Dimensional Soil-Structure Interaction Problems in the Time Domain, *Engineering Computations*, Vol. 1, No. 4, Dec. 1984, Pg. 298-311
3. Concus, P., G.H. Golub, and D.P. O'Leary, 1976, A Generalized Conjugate Gradient Method for the Numerical Solution of Elliptic Partial Differential Equations, in *Sparse Matrix Computations*, J.R. Bunch and D.J. Rose, Editors, Academic Press, New York
4. Herrmann, L.R., Y.F. Dafalias, and J.S. DeNatale, 1981, Bounding Surface Plasticity for Soil Modeling, Civil Engineering Laboratory, Naval Construction Battalion Center, Report CR 81.008
5. Herrmann, L.R., V.N. Kaliakin, and Y.F. Dafalias, 1983, Computer Implementation of the Bounding Surface Plasticity Model for Cohesive Soils, Dept. of Civil Engineering Report, The University of California at Davis
6. Herrmann, L.R., V.N. Kaliakin, C.K. Shen, K.D. Mish, and Z. Zhu, 1987, Numerical Implementation of Plasticity Model for Cohesive Soils, *ASCE Journal of the Engineering Mechanics Division*, Vol. 113, No. 4, April, 1987, Pg. 500-519
7. Herrmann, L.R., and K.D. Mish, 1983, Finite Element Analysis for Cohesive Soil, Stress and Consolidation Problems Using Bounding Surface Plasticity Theory, Civil Engineering Laboratory, Naval Construction Battalion Center, Report N62583-83-M-T062
8. Hughes, T.J.R., R.M. Ferencz, and J.O. Hallquist, 1986, Large-Scale Vectorized Implicit Calculations in Solid Mechanics on a Cray X-MP/48 Utilizing EBE Preconditioned Conjugate Gradients, *Computer Methods in Applied Mechanics and Engineering*, Vol 61, Pg. 215-248
9. Lanczos, C., 1950 An Iteration Method for the Solution of the Eigenvalue Problem of Linear Differential and Integral Operators, *Journal of Research of the NBS*, Vol. 45, No. 4, October 1950, Pg. 255-282
10. Mish, K.D., and L.R. Herrmann, 1987, The Solution of Large Nonlinear Time-Dependent Problems Using Reduced Coordinates, Civil Engineering Laboratory, Naval Construction Battalion Center, Report N68305-5345-3995
11. Nour-Omid, B., and B.N. Parlett, 1985, Element Preconditioning Using Splitting Techniques, *SIAM Journal of Scientific and Statistical Computing*, Vol. 6, No. 3, Pg. 761-770
12. Nour-Omid, B., B.N. Parlett, and R.L. Taylor, 1983, A Newton-Lanczos method for Solution of Non-linear Finite Element Equations, *Computers & Structures*, Vol 16, No. 1-4, Pg. 241-252

13. Parlett, B.N., 1980a, A New Look at the Lanczos Algorithm, Linear Algebra and Its Applications, Vol. 29, Pg. 323-346
14. Wilson, E.L., M. Yuan, and J.M. Dickens, 1982, Dynamic Analysis by Direct Superposition of Ritz Vectors, Earthquake Engineering and Structural Dynamics, Vol. 10, Pg. 813-821
15. Wilson, E.L., and Bayo, E.P., 1986, Use of Special Ritz Vectors in Dynamic Substructure Analysis, ASCE Journal of Structural Engineering, Vol. 112, No. 8, August 1986
16. Zienkiewicz, O.C., 1977, The Finite Element Method, McGraw-Hill, London
17. Zienkiewicz, O.C., and T. Shiomi, 1984, Dynamic Behavior of Saturated Porous Media; The Generalized Biot Formulation and its Numerical Solution, International Journal for Numerical and Analytical Methods in Geomechanics, Vol. 8, Pg. 71-96

DISTRIBUTION LIST

ARMY CORPS OF ENGRS HQ, DAEN-ECE-D (Paavola), Washington, DC
 ARMY EWES WESIM-C (N. Radhadrishnan), Vicksburg, MS
 DOT Dr. Pin Tong, Cambridge, MA
 DTIC Alexandria, VA
 DTRCEN Code 1720, Bethesda, MD
 GIDEP OIC, Corona, CA
 NAVFACENGCOM Code 04B2 (J. Cecilio), Alexandria, VA; Code 04BE (Wu), Alexandria, VA; Code 04R, Alexandria, VA
 NAVFACENGCOM - CHES DIV, FPO-IPL, Washington, DC
 NAVFACENGCOM - LANT DIV, Library, Norfolk, VA
 NAVFACENGCOM - NORTH DIV, Code 04AL, Philadelphia, PA
 NAVFACENGCOM - PAC DIV, Library, Pearl Harbor, HI
 NAVFACENGCOM - SOUTH DIV, Library, Charleston, SC
 NAVFACENGCOM - WEST DIV, Code 04A2.2 (Lib), San Bruno, CA
 NORDA Code 360, Bay St. Louis, MS
 NRL Code 4430 (Ramberg), Washington, DC
 NUSC DET Code 44 (Carlsen), New London, CT
 OCNR Code 1132SM (A.J. Tucker), Arlington, VA
 PWC Code 101 (Library), Oakland, CA; Code 123-C, San Diego, CA; Code 420, Great Lakes, IL; Library (Code 134), Pearl Harbor, HI; Library, Guam, Mariana Islands; Library, Norfolk, VA; Library, Pensacola, FL; Library, Yokosuka, Japan; Tech Library, Subic Bay, RP
 GEORGIA INSTITUTE OF TECHNOLOGY Mech Engrg (Fulton), Atlanta, GA
 NORTHWESTERN UNIV CE Dept (Belytschko), Evanston, IL
 OHIO STATE UNIVERSITY CE Dept (Sierakowski), Columbus, OH
 OREGON STATE UNIVERSITY CE Dept (Leonard), Corvallis, OR
 PENNSYLVANIA STATE UNIVERSITY Arch Engrg Dept (Geschwindner), University Park, PA
 PORTLAND STATE UNIVERSITY Engrg Dept (Migliori), Portland, OR
 RUTGERS UNIVERSITY CE Dept (Hanaor), Piscataway, NJ
 SOUTHERN ILLINOIS UNIVERSITY CE & Mech Dept (Kassimali), Carbondale, IL
 STANFORD UNIVERSITY App Mech Div (Hughes), Stanford, CA
 UNIVERSITY OF CALIFORNIA CE Dept (Herrmann), Davis, CA; CE Dept (Kutter), Davis, CA; CE Dept (Romstad), Davis, CA; CE Dept (Shen), Davis, CA; CE Dept (Taylor), Berkeley, CA; Geotech Model Cen (Cheney), Davis, CA; Mech Engrg Dept (Armand), Santa Barbara, CA; Mech Engrg Dept (Bayo), Santa Barbara, CA; Mech Engrg Dept (Bruch), Santa Barbara, CA
 UNIVERSITY OF COLORADO CE Dept (Hon-Yim Ko), Boulder, CO
 UNIVERSITY OF CONNECTICUT CE Dept (Murtha-Smith), Storrs, CT
 UNIVERSITY OF FLORIDA CE Dept (Townsend), Gainesville, FL
 UNIVERSITY OF HOUSTON CE Dept (K.J. Han), Houston, TX
 UNIVERSITY OF ILLINOIS CE Lab (Abrams), Urbana, IL; CE Lab (Pecknold), Urbana, IL
 UNIVERSITY OF MARYLAND CE Dept (Goodings), College Park, MD
 UNIVERSITY OF NEW MEXICO HL Schreyer, Albuquerque, NM
 UNIVERSITY OF SOUTH CAROLINA Engrg Coll (Karabalis), Columbia, SC
 ADINA ENGRG, INC Walczak, Watertown, MA
 ARMSTRONG AERO MED RSCH LAB Owenshire, Wright-Patterson AFB, OH
 CANADA Univ of Calgary (Glockner), Calgary, Alberta
 LEV ZETLIN ASSOC, INC DA Cuoco, New York, NY
 LOCKHEED Rsch Lab (Nour-Omid), Palo Alto, CA
 MARC ANALYSIS RSCH CORP Hsu, Palo Alto, CA
 PMB SYS ENGRG, INC S. Nour-Omid, San Francisco, CA
 SRI INTL Engrg Mech Dept (Simons), Menlo Park, CA
 TRW INC Crawford, Redondo Beach, CA; M Katona, San Bernardino, CA
 UNITED KINGDOM Univ Coll Swansea (Zienkiewicz), Wales
 WEIDLINGER ASSOC F.S. Wong, Palo Alto, CA
 BIRNSTIEL, C Forrest Hills, NY
 COX, J Davis, CA
 WEBSTER, R Brigham City, UT